



Comparison of the structural and electronic properties of two cobalt perovskites, in which Co is formally d^6 (LaCoO_3), and d^7 (KCoF_3)

Alexander Platonenko¹, Khaled E. El-Kelany^{2*}, Julio Sambrano³, Klaus Doll⁴, Roberto Dovesi⁵

¹Institute of Solid State Physics, University of Latvia, 8 Kengaraga street, LV1063, Riga, Latvia,

²Institute of Nanoscience and Nanotechnology, Kafrelsheikh University, 33516 Kafr el-shiekh, Egypt,

³Facultate de Ciencias, Sao Paulo State University, Bauru, Brasil,

⁴University of Stuttgart, Molpro Quantum Chemistry Software, Institute of Theoretical Chemistry, Pfaffenwaldring 55, D-70569 Stuttgart (Germany),

⁵ACCADEMIA DELLE SCIENZE DI TORINO, Via Accademia delle Scienze 6, 10123 Torino (To), Italy

*Correspondence: khaled.elkelany@nano.kfs.edu.eg, ORCID: 0000-0001-8216-8496

Abstract

Background: The electronic and geometrical properties of LaCoO_3 , which has a closed shell ground state ($S_z=0$), are compared with the ones of KCoF_3 , presenting a high spin ($S_z=3/2$) ground state. In an ideal fully ionic model, the Co occupancy in the two compounds is d^6 (oxide) and d^7 (fluoride).

Methods: The analysis of the density of states and of the charge distribution, the latter through a Mulliken analysis, shows that in the oxide the partially covalent character of the Co-O bonds deeply alters the ideal picture, and that not only the t_{2g} , but also the e_g subshell is occupied, with an overall d occupancy close to 7 electrons (one electron in the e_g subshell), very close to the fluoride occupancy.

Results and conclusion: The deformation with respect to the cubic *aristotype* (SG 221), down to the tetragonal (SG 123, 127 and 140), orthorhombic (SG 62) and rhombohedral (SG 167) symmetry, with a corresponding increase of the inner degrees of freedom (from 1 to 10) and size of the unit cell (from 5 to 20 atoms), is explored, which confirms that the octahedra remain essentially regular, with an energy gain along the full group-subgroup chain of only 4.6 mE_h (0.125 eV) per formula unit. In spite of the similar total occupancy of the d shell, the electronic configuration of Co in KCoF_3 is quite different, with a high spin ($t_{2g}^5 e_g^2$, with 5α and 2β electrons) ground state.

Keywords: LaCoO_3 and KCoF_3 perovskites, B3LYP, Mulliken analysis, d orbital occupancy, octahedra rotation, DOS.

1. Introduction

In the fully ionic representation, or according to the empirical *oxidation numbers*, the atomic charges in the LaCoO_3 perovskite are +3(La), +3(Co) and -2(O). The corresponding formal charges for KCoF_3 are +1(K), +2(Co) and -1(F). This would correspond, for the common cobalt transition metal, to the $1s^2 2s^2 2p^6 3s^2 3p^6 3d^7$ configuration in the fluoride (only the two 4s electrons of the neutral atom are lost); in the oxide, also one of the d electrons is supposed to be lost, resulting in a d^6 occupancy. The high spin configuration ($S_z=3/2$, quadruplet) turns out to be the ground state for the d^7 case: $t_{2g}^5 e_g^2$, with 5α and 2β electrons; for the formally d^6 oxide case, the closed shell t_{2g}^6 , $S_z=0$ state turns out to be the ground state.

This ionic picture is however an extreme point of

view, not taking into account chemical aspects such as the amount of covalent degree of the bonds (certainly higher in the oxides, but: how much?) which might alter the above simplified analysis.

In the present paper we analyze the electronic structure (as well as the geometrical parameters) of LaCoO_3 in its ground state, and compare them with the KCoF_3 ones (see also Refs [1, 2]).

In particular, through a Mulliken analysis, we discuss if and how the fully ionic model is a reasonable representation of the charge distribution in the oxide and in the fluoride.

A second crucial aspect of the present investigation is the relative stability obtained by imposing different symmetry constraints in the optimization process. We will start imposing the

cubic symmetry (space group Pm-3m, space group number 221), in which only the lattice parameter is allowed to change. Then, progressively, we will follow the group-subgroup chain to SG $P\frac{4}{m}mm(123)$, and then $P\frac{4}{m}bm(127)$ and finally Pbnm (62). At each passage, the degrees of freedom in the optimization path increase (from 1 to 10) as well as the number of formula units (f.u.) (from 1 to 4). Parallel branches to SG $I\frac{4}{m}cm(140)$ and SG R-3c (167) will also be explored, and the energy gain and geometrical modifications will be commented. A similar path will be followed for KCoF₃, which permits to underline the large differences between the Co oxide and fluoride.

LaCoO₃ is particularly interesting, because of its unusual magnetic behavior originating from the balance between the crystal field effect and the intra-atomic (Hund's-rule) exchange. In the ground state LaCoO₃ is a non-magnetic insulator: Co³⁺ is formally 3d⁶, producing the low-spin (LS; t_{2g}⁶) configuration.

A spin transition is however observed at about 100 K from the non-magnetic LS state to a magnetic state which was considered to be the high-spin (HS) t_{2g}⁴e_g² state. There are several discrepancies in the interpretation of the nature of this state: also an *intermediate spin state* (IS) t_{2g}⁵e_g¹ seems to be present above 100 K. It is then not surprising that LaCoO₃ has been the object of many experimental [7, 8, 9, 10, 11, 12, 13] determinations in various T ranges. In the present manuscript we will limit our investigation to the LS t_{2g}⁶ state, to which most of the theoretical [14, 15, 16, 17, 18, 19, 20] investigations refer. This analysis will be followed, in a forthcoming paper, by the investigation of the lowest energy excited states, using the Δ -SCF computational scheme already applied by some of the present authors for the investigation of the excited states of NiO [3], Al₂O₃ [4], and defects in diamond (vacancy [5],

vacancy plus substitutional nitrogen couple [6]).

As regards the structure of LaCoO₃, Thornton *et al.* [7] (1986) performed neutron diffraction experiments in a large temperature interval (4 to 1248 K), and suggested space group R-3c (N. 167) though for one temperature marginal evidence for R-3 (N. 148) was observed. A few years later (2004), Haas *et al.*, on the basis of various X-ray techniques [8], suggested the space group R-3c (N. 167) as the structure at 700 K, or possibly its subgroup I2/a (N. 15)

Arima *et al.*, in 1993, investigated the nature of the band gap in a large family of perovskites ABO₃, including LaCoO₃, for which "the effects of the M-3d – O-2p hybridization must be included". As we will see, the proposed band gap is much smaller than the largest part of the simulated ones resulting from the DOS of the ground state.

On the side of simulation, the equilibrium geometry is usually explored, considering only the R-3c SG, as proposed by the most recent experiment [8]. In their systematic investigation of the full LaBO₃ family (B = Sc to Cu), He and Franchini [21, 22, 23] assumed the R-3c structure for LaCoO₃. A large variety of functionals has been used, ranging from pure LDA [16, 19] to LDA+U (with various U values [18, 15, 20]) and the full range hybrid PBE0 [19]. Also GW [17] and HF [14] calculations have been proposed.

All these studies are quoted in the already mentioned extended paper by He and Franchini [21, 22, 23], who adopted the PBE and the HSE functionals, the latter with various values of the mixing parameter for the exact Hartree-Fock exchange.

The present paper is structured as follows: in section 2, the computational conditions are defined. In section 3 the results are presented, followed by a discussion and some conclusions in section 4.

763311(631)G, 8-6411(51d)G and 8-411(1)G contractions, consisting of 1s, 6sp and 3d shells (40 atomic orbitals, AOs) for La, of 1s, 4sp and 2d shells, (27 AOs) for Co, and of 1s, 3sp and 1d shells (18 AOs) for oxygen, for a total of 121 AOs

2. Computational Details

The ferromagnetic solutions for the LaCoO₃ and KCoF₃ compounds have been evaluated at the B3LYP [24, 25] level by using the CRYSTAL code [26, 27, 28]. The triple zeta type 9-

per formula unit, have been used in the case of LaCoO₃. For KCoF₃ the contractions are 7-311G and 8-6-511G for F and K (13 and 17 AOs); for Co, the same contraction is used as in the oxide. Exponents and coefficients of the basis set have been optimized in the bulk.

The Coulomb and Hartree-Fock exchange series are controlled by five parameters [26] that were set to T1=T2=T3=T4 and T5=2xT1, with T1=10 (for a complete description of the role of these parameters see also Refs. [29, 30]); these values are required for an accurate evaluation of the small differences between the various phases of the

system, ranging between 10⁻³ and 10⁻⁵ E_h. As regards the DFT exchange-correlation contribution to the Fock matrix, it was evaluated by numerical integration over the unit cell volume. Radial and angular points for the integration grid were generated through a Gauss-Legendre radial quadrature and Lebedev two-dimensional angular point distributions. In the present work, a pruned grid with 99 radial and 1454 angular points was used (see XXLGRID keyword in the CRYSTAL manual [26]). All calculations have been performed by using a supercell of the primitive cell, containing one, two or four magnetic centers.

Table 1: Variation of the total energy E (in E_h), cell volume (in Å³) and band gap (in eV) of the LaCoO₃ and KCoF₃ perovskites, as a function of the adopted space group. In the fully ionic description, the formal occupancy is d⁶ (t_{2g}⁶) for the oxide, and d⁷ (t_{2g}⁵e_g²) for the fluoride. In SG 221 and 123 the unit cell contains 1 f.u.; in SG 127 and 140, and 167, 2 f.u.; in SG 62, 4 f.u. The energies and volumes are per f.u. ΔE (in mE_h) is the difference with respect to the total energy of SG 123. In SG 127 and 140 the octahedra are allowed to rotate with respect to one axis, in SG 62 they can rotate with respect to three axes and the d occupancy on B can flip from site to site (this applies to the fluoride case, with partial occupancy). In SG 167 the apical angle of the octahedra can deform. In the case of SG 140D, also the AFM data are reported.

	SG	E	ΔE	V	Gap
LaCoO ₃	Pm-3m (221)	-9832.377967	0.0	57.182	2.33
	P _m ⁴ -mm (123)	-9832.377967	0.0	57.182	2.33
	P _m ⁴ -bm (127)	-9832.378592	-0.6	57.461	2.36
	I _m ⁴ -cm (140)	-9832.381335	-3.4	57.636	2.46
	Pbnm (62)	-9832.382245	-4.3	57.813	2.54
	R-3c (167)	-9832.382446	-4.5	57.834	2.55
KCoF ₃	Pm-3m (221) FM	-2282.307514	+46.9	70.173	3.93
	P _m ⁴ -mm (123)* FM	-2282.353754	+0.6	70.173	3.93
	P _m ⁴ -mm (123)	-2282.354387	0.0	70.171	3.92
	I _m ⁴ -cm (140R) FM	-2282.354390	0.0	70.171	3.92
	I _m ⁴ -cm (140D) FM	-2282.355162	-0.8	70.174	3.93
	Pbnm (62) FM	-2282.355162	-0.8	70.174	3.93
	I _m ⁴ -cm (140D) AFM	-2282.356478	-2.1	69.823	4.45

3. Results

In the fully ionic picture of LaCoO₃ (La³⁺, O²⁻, Co³⁺), the d occupancy of Co is expected to be t_{2g}⁶ (the two 4s and one of the d electrons are lost, to give Co³⁺), compatible with the cubic symmetry. The effect of the reduction of the SG from cubic (N. 221) to tetragonal (123, 127 and 140), rhombohedral (167) and finally to orthorhombic (62), is shown in Table 1 (data refer to one formula unit, f.u., 5 atoms in the unit cell). Reducing the point symmetry, and increasing the number of f.u.

in the unit cell, increases also the degrees of freedom in the geometry optimization process, as shown in Table 4 for the involved SGs (see also the Appendix). In the t_{2g}⁶ configuration of Co, the Jahn Teller splitting (JTS) and orbital ordering (OO) mechanisms are then not active, so that the deformation of the cell, if any, is to be attributed to the relative size of the three ions. The value of the tolerance factor t for LaCoO₃ and KCoF₃, when the Shannon [31] ionic radii are used, is very close to 1.0, suggesting that the octahedra deformation, if

any, is quite small (see also the values in Figure 25 of the He and Franchini paper [21]). Table 4 shows that in SG 221 and 123 (1 f.u./cell in both cases), all atoms are in special position, and in the optimization process only the *a* (SG 221) or *a* (= *b*) and *c* (SG 123) lattice parameters are allowed to vary. Table 1 shows that the additional freedom of SG 123 with respect to the cubic case is not exploited, as expected. In SG 127R (see Appendix for the meaning of R), with two f.u./cell (10 atoms), the oxygen ion in the *ab* plane can move, in such a way that the octahedra rotate with respect to the *c* axis. In SG 140R, contiguous octahedra along *c* can rotate in opposite directions. The energy gains with respect to SG 221 are 0.6 and 3.4 mE_h, respectively. The further reduction of point symmetry, and increase of unit cell size in SG 62 (4 f.u./cell, 10 geometrical degrees of freedom in the optimization process, see Table 4) permits a further energy gain of 0.9 mE_h per f.u.. SG 62 is a local minimum, as verified by the vibrational frequencies, which are all positive. The overall energy gain from the perfect cubic structure is then 4.3 mE_h (about 0.12 eV).

When the alternative deformation to SG R-3c is allowed, the energy gain is just slightly larger, by 0.2 mE_h (4.5 vs 4.3 mE_h). These energy differences are more than two orders of magnitude larger than the ones observed for KCoF₃, shown in the lowest part of Table 1, the exception being the passage from the cubic case (SG 221, metallic solution, due to the partial occupancy of the *t*_{2g} subshell with 5 electrons in 6 holes), to SG 123, in which the 3 *t*_{2g} orbitals split in two sets, with two of them (say *d*_{xz} and *d*_{yz}) doubly occupied, and one (say *d*_{xy}) singly occupied; in this case the energy gain is as large as 46.9 mE_h (at fixed volume, the one optimized for the cubic solution); the further relaxation of the *a* and *c* lattice parameters reduces the energies by only 0.6 mE_h. The JTS is then the dominant mechanism in the KCoF₃ case.

The optimized structure and energy with SG 127R and 140R coincide with the ones of SG 123: this means that in KCoF₃ the octahedra are not rotating. In SG 140D (see Appendix) there is a gain of 0.8 mE_h per f.u., due to the different occupancy of the Co *d* shell in contiguous Co atoms in the *ab* plane. This point is discussed at length by some of the present authors in two recent publications [32, 2]

devoted to the orientations of the occupied *d* orbitals on the 8 B (B= Sc, Ti, Fe and Co) atoms in a 2x2x2 supercell (containing then 8 B atoms) of KBF₃. All possible different configurations (6561, grouped in 162 symmetry equivalent classes), have been optimized and their energy ordered. We can summarize the results shown in Table 1, as follows: For KCoF₃, the JTS is by far the largest effect as regards the energy. JTS is null for LaCoO₃.

a) There is no octahedra rotation (OR) in KCoF₃. In LaCoO₃ it accounts for about 3.4 mE_h per f.u.

b) We have been unable to observe any orbital ordering effect in the oxide, whereas in the fluoride it accounts for about 0.8 mE_h per f.u.

c) In the oxide, SG 167 and 62 are nearly equi-energetic. The experimental determinations, dating back to 1986 [7] and 2004 [8], attribute the lowest energy structure to SG 167 (or to its subgroup R3c, N 161), both at low and room temperature. This is a quite reasonable choice, being the symmetry of SG 167 higher than the one of SG 62 (see Table 4). The present results suggest however that also the orthorhombic structure might be proposed (it should be underlined that SG 62 is NOT a subgroup of SG 167, so that it is not possible to pass from one to the other by simply attributing to the experimental numerical noise the deviation of some fractional coordinates from the values corresponding to special positions, as it is possible for increasing the symmetry from a subgroup to its parent).

d) The gap for the oxide, 2.54 eV, is only 1.4 eV smaller than for the fluoride, which is expected to be much more ionic.

The volume of the oxide is much smaller than the one of the fluoride, due to electrostatics (formal charges of the anions 2- and 1-, so the Coulomb forces are 4 times larger for the oxides), and larger covalent character.

In Table 2 some of the geometrical parameters for three equilibrium structures of LaCoO₃ are shown, whereas the equilibrium volume *V* for all explored SG is given in Table 1. The volume *V* confirms the energy data, with a maximum percentage difference as small as 1.12% in going from the cubic case, with the smallest volume, to the rhombohedral case, with the largest one (57.18 vs 57.83). As for the energy, the orthorhombic (SG 62) and rhombohedral (SG 167) volumes are

extremely close (0.021 Å³ difference). Both the energy and volume changes are very small numbers. The regular trends in Table 1 confirm that the numerical accuracy of the CRYSTAL code is very high also for energy differences of the order of 1-2 mE_h. Looking at Table 2, we can estimate the deformation of the Co-O₆ octahedron, and La-O₁₂ dodecahedron. The six Co-O distances are the same by symmetry both in SG 221 and 167 (1.926 and 1.953 Å); in SG 62 they split into three sets, but the differences are on the third decimal figure:

1.951 vs 1.955 Å. So the maximum difference in the three cases is 0.03 Å (1.926 vs 1.955 Å). Much larger is the deformation of the La-O dodecahedron: it is regular (2.724 Å) for SG 221; it splits in three sets of 3, 6 and 3 members in SG 167, with La-O distances spanning about 0.5 Å (2.476, 2.731, 3.030 Å); in the orthorhombic case they span nearly one Angstrom (the first 9 neighbors are shown in the table). In spite of these deformations, as already mentioned, the energy differences are within 0.12 eV/f.u.

Table 2: Equilibrium geometry of various space groups of LaCoO₃ in the low spin configuration: lattice parameters (in Å), volume (in Å³) and atom-atom distances (in Å). B3LYP solution. The numbers in parentheses indicate how many distances coincide.

	LaCoO ₃		
	R-3c (167)	Pbnm (62)	Pm-3m (221)
a	5.4334	5.5164	3.8525
b	5.4334	5.4324	3.8525
c	5.4334	7.7168	3.8525
α	60.878	90.0	90
β	60.878	90.0	90
γ	60.878	90.0	90
V	57.834	57.813	57.182
Co-O	1.953(6)	1.951(2)	1.926(6)
	--	1.951(2)	--
	--	1.955(2)	--
Co-La	3.305(2)	3.296(2)	3.336(8)
	3.364(6)	3.420(2)	--
	--	3.475(2)	--
La-O	2.476(3)	2.420(1)	2.724(2)
	2.731(6)	2.513(2)	
	3.030(3)	2.566(1)	
	---	2.688(2)	
	--	2.840(2)	
	--	3.121(1)	

3.1. The density of states

The density of states (DOS) of LaCoO₃ for four different SGs (221, 127, 167 and 62) is shown in Figure 1, where in the valence region only the O p and the Co d states appear. The La 5s states are at about -32 eV, and the 5p states at -18 eV, quite close to the O 2s states, at -20 eV. The 3s and 3p Co states are much deeper, at -100 and -65 eV, respectively (energies refer to the top of the valence band; note also that the *all electron* basis set permits to locate inner states, and avoids artefacts due to pseudopotentials). All these bands result in sharp peaks in the DOS, with no dispersion in reciprocal space, as they do not

overlap with neighbors.

Only the Co d orbitals contribute to the bottom part of the conduction band, shown in the figure. The mixed charge transfer (CT, from oxygen to Co d e_g states) and Mott-Hubbard (MH, from Co t_{2g} to Co e_g) nature of the electronic transition, as emerging from the DOS, is evident from the figure, and confirms the usual indication (see for example [21]).

The band gap of the most stable structure is 2.55 eV (SG 167 and 62); for SG 221 and 127 it is very similar, 2.33 and 2.36 eV, confirming that the structure of LaCoO₃ remains quite close to the cubic one, with minor deformations. It should be

noted that in the figures the attribution of the states to the t_{2g} and e_g subshells is correct only for the higher symmetry groups, 221 and 123, in which the cartesian x, y and z axes are aligned along a, b and c. In the other cases the octahedra slightly deform or rotate, so that the two subsets mix to a given amount. This point is however irrelevant for the present discussion.

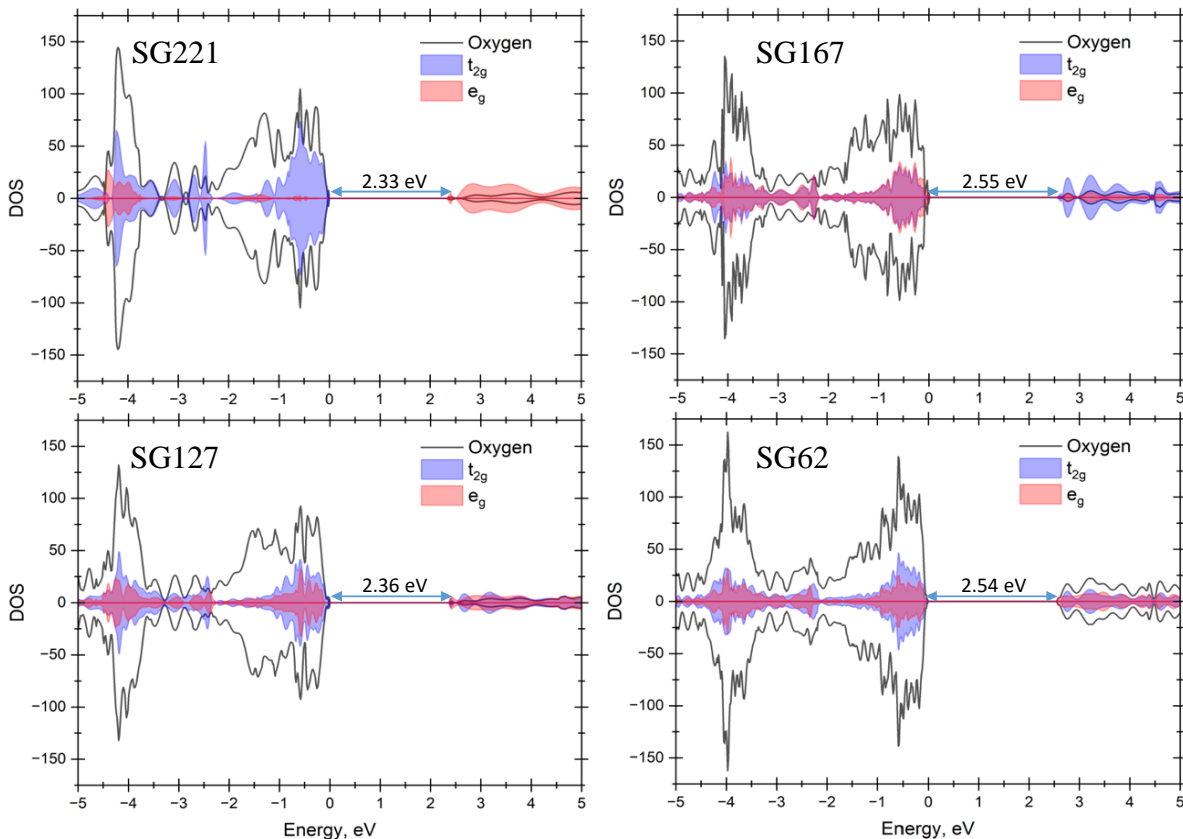
The calculated band gap of 2.55 eV is much larger than the one reported as “the experimental gap” [21, 22, 23], which is as small as 0.1 [21] or 0.3 [9]. The calculated gaps available in the literature range between 0.0 and 1.06 eV [16, 19] when the pure LDA is used, between 0.1 and 2.1 eV [18, 15, 20] when LDA+U (with various U values), is adopted; it is 2.5 eV [19] with the full range hybrid PBE0 functional, and 1.28 eV [17] with GW; finally, 3.5 eV is reported when HF [14] is used.

It is not clear whether the different values reported in the literature reflect mainly the adopted functional, or theoretical approach, or are affected to a large amount also by the other features of the

method, including the kind and extension of the basis set and the numerical accuracy in the various steps of the calculation. As a partial answer to this question, we repeated the calculation for the lowest energy structure, corresponding to SG 167, with pure LDA, PBE, PBE0, and HF, for which other calculations are available. The gaps we obtained differ in most of the cases from the ones tabulated by He and Franchini [21]. For LDA and PBE we obtained a metallic solution. At the other extreme, for HF we obtained 13.2 eV, much larger than the one reported by Mizokawa [14], only 3.5 eV. It is clear that Mizokawa’s gap is largely underestimated, as for small-gap insulators, an accurate HF scheme produces gaps which are ten times, or even more, larger than full range or range separated hybrids. For example, in the LaTiO₃ case, the gaps we obtained [33] are 0.3 (B3LYP), 0.6 (PBE0), 11.3 (HF).

We can conclude that the indication of the adopted method is not enough for guessing the results one can obtain, as all the other aspects of the method can play a crucial role.

Figure 1: Density of states (DOS, in arbitrary units) of LaCoO₃ for four different space groups: cubic (SG 221), tetragonal (SG 127), orthorhombic (SG 62) and rhombohedral (SG 167). The continuous line indicates the p states of O. The t_{2g} and e_g d states of Co are in blue and pink, respectively. Note however that only in SG 221 the cartesian axes x, y and z coincide with the a, b and c lattice parameters, so that the directions of the lobes of the 5 d orbitals coincide with the crystallographic axes. In the other cases the correspondence is in part lost, due to the rotation and deformation of the octahedra.



Let us consider now KCoF_3 , whose DOS is shown in Figure 2, for SG 123 FM, 140 FM and AFM solutions. In this case three projections are shown. The figures suggest the following comments:

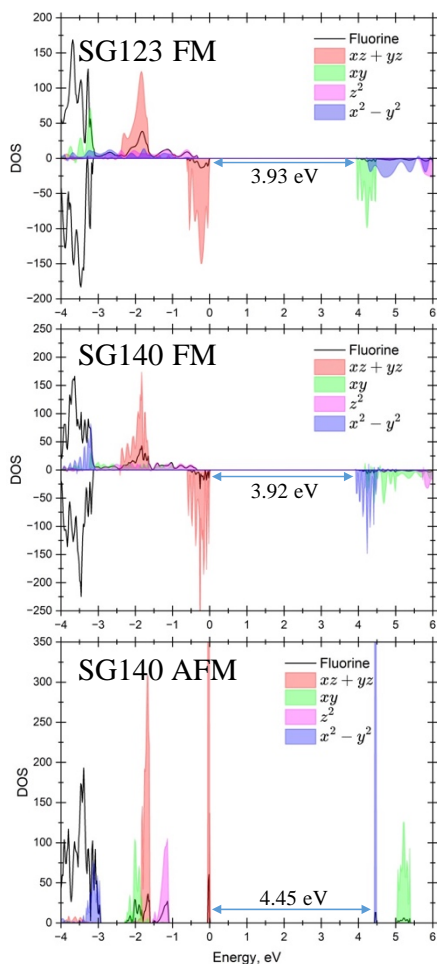
- The main difference with respect to LaCoO_3 , is that fluorine is not contributing at all to both the valence and conduction bands, so the transition is Co to Co, or Mott-Hubbard in nature.
- In the SG 123 case, where the octahedra principal axes are along the a , b and c lattice parameters, the transition is t_{2g} to t_{2g} (more specifically, from $d_{xz}+d_{yz}$ to d_{xy} , with $d_{x^2-y^2}$ being slightly higher in energy). The gap is 3.93 eV.
- In SG 140 the octahedra rotate, so that d_{xy} and $d_{x^2-y^2}$ partially mix in the definition of the bottom

of the conduction band, which appears now mainly to be $d_{x^2-y^2}$. The nature of the gap remains however the same as for SG 123, and its value is the same too (3.92 eV).

- As usual, the AFM solution provides much sharper bands, due to the reduced dispersion in reciprocal space, in turn due to the reduced Pauli repulsion between one Co and its first neighbours (see Reference [34]). As a result, the gap increases by 0.52 eV.

In summary, the main, crucial difference between the oxide and the fluoride compounds is that the anion bands in the latter are deeper in energy, and do not participate at all to the valence and conduction bands.

Figure 2: Density of states (DOS, in arbitrary units) of KCoF_3 for space SG 123 FM, 140 FM, 140 AFM (from top to bottom). In the AFM case only the positive part of the DOS is shown, as the figure is symmetric with respect to the horizontal axis. The continuous line indicates the p states of F. The t_{2g} d states of Co are split in two sets, $d_{xz} + d_{yz}$, and d_{xy} . Similarly, the e_g states are split in d_{z^2} and $d_{x^2-y^2}$ for a better classification. Note that under rotation with respect to the c axis (SG 140), d_{xz} and d_{yz} mix, as well as d_{xy} and $d_{x^2-y^2}$.



3.2. The charge density and the Mulliken analysis

The net charges Q , obtained from a Mulliken analysis applied to the charge and spin density functions, are shown in Table 3, for the FM and the AFM (KCoF_3 only, as LaCoO_3 is closed shell) solutions, and refer to the B3LYP functional. In the ideal fully ionic picture, Q for Co is expected to be $+3 |e|$ in the oxide, and $+2 |e|$ in the fluoride. This is not the case, however, with a reduction of ionicity in the oxide of $+1.26 |e|$ (or 42%: from $3.00 |e|$ to $1.74 |e|$); for the fluoride the reduction is of only $0.35 |e|$ (or 18%: from $2.00 |e|$ to $1.65 |e|$). The ionicity of the other cation is quite close to the ideal value (with a reduction of the charge of $3.00-2.70 = 0.30 |e|$ for La (10%), and of $1.-0.92 = 0.08 |e|$ for K; 8%). The reduction of the Co ionicity with respect to the ideal value, is fully compensated by the corresponding reduction of the anion: $-1.49 |e|$ instead of $-2.00 |e|$ (26%) for the oxygen, and $-0.87 |e|$ instead of $-1.00 |e|$ (13%) for F. As expected, the fluoride is much closer to the ideal ionic limit than the oxide.

The positive bond population data for the oxide indicates that there is a fraction of covalent bond between Co and O ($+0.045 |e|$, that when multiplied by 6, the number of Co-O neighbors, shows that about 1/4 of an electron is shared between Co and O). B is null between La and Co, repulsive (negative) between La and O, and between O first neighbors of Co.

When looking at the population of the d shell (see

the d shell entry in the table), we observe that it is close to $7 |e|$: there are seven electrons in the d shell of Co in both compounds. The spin population of the Co d shell in KCoF_3 (last column of Table 3) is close to $3 |e|$, indicating that there are 3 unpaired electrons, corresponding to the 5α and 2β occupancy: $t_{2g}^5(3\alpha$ and $2\beta)$ plus $e_{2g}(2\alpha)$.

The information concerning which one of the 5 d orbitals is occupied, and which one is not, can be obtained only when the orientation of the cartesian axes and of the a , b and c lattice parameters coincide. This is the case of SG 221, where we observe that not only the three t_{2g} orbitals are doubly occupied, but that one additional electron populates both e_g orbitals (about $0.6 |e|$ on both).

In SG 62 the numbers are similar (apart from permutations). The situation of SG 167 is slightly more confused, but the overall occupancy is the same as in the two other SGs. The overall occupancy of the d shell of cobalt in KCoF_3 , as already mentioned, is the same (about 7 electrons) as in LaCoO_3 . In this case, however, each orbital contains 2 or 1 electron, generating the $S_z = 3/2$ solution.

In summary, the ideal ionic Co^{3+} charge is only vaguely close to the real situation: Co does not lose the two 4s plus one of the d electrons. It is rather $\text{Co}^{1.47+}$, where the d shell maintains its 7 electrons as in the isolated atom, and the two 4s electrons are only partially lost, and partially shared with the oxygen first neighbors.

Table 3: Atomic net changes Q, population of the d shell of the Co atom, of the individual d orbitals, and atom-atom bond populations B obtained from a Mulliken analysis. X stands for O or F, A stands for La or K. B3LYP results. The LaCoO_3 ground state is a closed shell, $S_z=0$, t_{2g}^6 on Co. The KCoF_3 ground state is the high spin solution, $S_z=3/2$, $t_{2g}^5 e_g^2$ on Co. $\alpha+\beta$ indicates the total charge density, $\alpha-\beta$ is the corresponding spin density.

	LaCoO ₃			KCoF ₃	
	$\alpha+\beta$	$\alpha+\beta$	$\alpha+\beta$	$\alpha+\beta$	$\alpha-\beta$
	R-3c	Pbnm	Pm-3m	I4/mcm	
Q _{Co}	+1.742	+1.743	+1.743	+1.65	± 1.64
QX	-1.481(6)	-1.488	-1.488	-0.865	+0.07
QA	+2.702	+2.702	+2.703	+0.92	+0.92
B(Co - X)	+0.045	+0.045(6)	+0.042	-	-
B(A - X)	-0.029	-0.034 (-0.016)	-0.001	0.0	0.0
B(X - X)	-0.025	-0.026	-0.026	-	-
B(A - Co)	0.00	0.00	0.0	0.0	0.0
d shell	7.073	7.071	7.071	7.185	2.810
d _{xy}	1.494	0.610	1.965	1.100	0.906
d _{xz}	1.060	1.903	1.965	1.993	0.002
d _{yz}	1.060	1.944	1.965	1.993	0.002
d _{z2}	1.965	0.650	0.588	1.072	0.929
d _{x2-y2}	1.494	1.964	0.588	1.027	0.971

4. Discussion and Conclusions

The equilibrium geometry and total energy of LaCoO_3 have been obtained by exploring the high symmetry cubic *aristotype* (SG $Pm\bar{3}m$, N. 221), in the closed shell low spin configuration with the B3LYP functional, and various subgroups according to the group-subgroup chains:

$$Pm\bar{3}m \text{ (N. 221)} \rightarrow P\frac{4}{m}bm \text{ (N. 127)} \rightarrow$$

$$I\frac{4}{m}cm \text{ (N. 140)} \rightarrow Pbnm \text{ (N. 62)}$$

and

$$Pm\bar{3}m \text{ (N. 221)} \rightarrow R\bar{3}c \text{ (N. 167)}$$

SG 221 contains 5 atoms in the unit cell, with 48 point symmetry operators; all atoms are in special position. In the other SGs the unit cell increases (up to a factor 4, in SG 62), the number of point symmetry operators reduces, and the degrees of freedom in the optimization process increase, as shown in Table 4. Table 1 shows that:

- 1) the most stable SG is $R\bar{3}c$ (N.167), in reasonable agreement with experiments [8, 7];
- 2) the energy of SG 62 is however quite close

to the one of SG 167 (only 0.2 mE_h difference, or 5.4 meV);

3) the overall gain with respect to the cubic aristotype is 4.48 mE_h (0.12 eV);

4) to the small energy gains from SG 221 to SG 167 correspond, as expected, very small volume and band gap variations,

5) so that the CoO₆ octahedra remain nearly regular, as shown in table 2. In SG 167, the most stable structure, the only deformation is the increase of the rhombohedral angles from 60.0° to 60.9°.

At variance with respect to LaCoO₃, in KCoF₃ (see the lowest part of Table 1), the most stable structure is the high spin configuration, with S_z=3/2.

In this case we observe:

1) The energy differences along the group-subgroup chain, from SG 123 to SG 140D, is even smaller than for the oxide.

2) Note however that there is a huge energy gain in going from SG 221 to SG 123, related to the Jahn Teller splitting (JTS) in the t_{2g} subshell, containing two electrons in three degenerate orbitals: the separation of the three levels in two and one levels generates an energy gain of 46.9 mE_h, by far the largest energy difference appearing in Table 1.

3) Another noticeable difference between the two compounds is that in the fluoride, the occupancy of the d orbitals changes on Co atoms which are symmetry related by a C₄ operator (let us suppose oriented along z): d_{xz} and d_{xy} transform in d_{yz} and d_{xy}, and so on. This is possible when SG 140D is used, in which the C₄ operator is at the center of a square (in the xy or ab plane) with 4 Co ions on the corners. The energy difference between SG 123 and SG 140D, due to the *flip* of

the d occupancy from site to site, or orbital ordering (OO), is 0.8 mE_h only. Both these mechanisms (JTS and OO) are obviously not active in LaCoO₃, which is low spin and closed shell.

The last point of interest discussed here is the adequacy of the full ionic representation in the two compounds, documented in Table 3. The Mulliken net changes of KCoF₃ are quite close to the ionic picture: +1.65 vs +2.00 |e| for Co, +0.92 vs +1.00 |e| for K, -0.87 vs -1.00 |e| for F. The d shell contains 7.07 electrons, with occupancy very close to 2 for d_{xz} and d_{yz}, and to 1 for the three other orbitals; this generates the high spin solution with S_z=3/2.

LaCoO₃ is on the contrary much farther from the ionic picture: the net charges are +1.74 vs +3.00 |e| for Co, +2.70 vs +3.00 |e| for La, and -1.49 vs -2.00 |e| for O. The Co d population is however very close to the one in KCoF₃ (7.19 vs 7.07 |e|), indicating that in the two compounds the d shell, which is quite internal, behave in a similar way; or, in other words, Co is not giving d electrons to the neighbors with respect to the isolated atom situation. It is rather from the 4s electrons that we have a partial donation to oxygen. This different ionic-covalent character of the oxide and fluoride is responsible for the different lowest energy state, which is low spin for LaCoO₃ (and consequently closed shell solution) and high spin in KCoF₃. In a forthcoming paper we will investigate the energy difference between these two situations (low and high spin) in the two compounds, by using the Δ-SCF scheme already applied by some of the present authors to the investigation of the excited states of NiO [3] and Al₂O₃ [4], and of various defects in diamond [5, 6].

Table 4: Information concerning some of the space groups used in this study.

SG(I)	SG(N)	Bravais	Z	N _f	free
Pm-3m	221	C	1	1	a
P4/mmm	123	T	1	2	a,c
P4/mbm	127	T	2	3	a,c, O ₁ (1)
I4/mcm	140	T	2	3	a,c, O ₁ (1)
R-3c	167	R	2	3	a,c, O ₁ (1)
Pbnm	62	O	4	10	a,b,c,O ₁ (3),O ₂ (2),K(2)

Label, SG(l), number, SG(N), Bravais lattice (C = cubic, T = tetragonal, O = orthorhombic, R=rhombohedral); Z is the number of formula units in the cell. N_f gives the number of degrees of freedom, listed in the *free* column, including the lattice parameters (1 for C, 2 for T and R, 3 for O) and the atomic fractional coordinates. O_1 and O_2 are oxygen atoms in the basal plane and along the *c* axis, respectively. $O_1(3)$ indicates that all three coordinates of the O_1 ion can vary.

5. Appendix

The definition of the space group (symbol, or number) does not define completely, in general, the kind of degrees of freedom within the unit cell. For each atom, the position must be defined through the *x,y,z* fractional coordinates. Consider the case of perovskites, for example LaCoO_3 . In the case of SG Pm-3m (N. 221), all atoms are in special position, so that the 48 point symmetry operators (PSO), which in principle might generate 48 La, Co and O atoms, actually transform in all cases La in itself, and Co in itself. As regards O, 16 PSO leave the O position (let us call it O_1) unaltered, 16 generate from O_1 a new O atom (O_2), and 16 generate O_3 . The number of atoms in the unit cell is then 5: one La, one Co and three O. For the definition of the unit cell, in CRYSTAL, it is sufficient to define the coordinates of La, Co and of one O, as the other two O atoms are generated by symmetry. In the optimization process only one parameter can be varied, because the PSOs transform *a* into *b* and *c*, so that they cannot be optimized independently, as documented in the first line of Table 4.

The CRYSTAL code, from the very first releases, exploited the point symmetry. The input for the generation of the infinite lattice, when the cubic symmetry (SG 221) is imposed, is very simple:

```
Line 1: 221
Line 2: 4.5200
Line 3: 3
Line 4: 27 0. 0. 0.
Line 5: 8 0.5 0. 0.
Line 6: 57 0.5 0.5 0.5
```

Six lines are sufficient for the complete definition of the geometrical input file, as described at length in the CRYSTAL manual [26]. Line 1 defines the group, line 2 the lattice parameter, line 3 the number of irreducible atoms, lines 4, 5 and 6 give the atomic number and the fractional coordinates of the 3 irreducible (i.e. non equivalent) atoms. They can be identified more precisely through the Wyckoff symbols.

When passing to SG $P\frac{4}{m}mm$ (N. 123), tetragonal, the number of PSO reduces to 16, *c* is no more symmetry related to *a* and *b*, but all atoms remain in special position. The unit cell contains also in this case 5 atoms, and the CRYSTAL input is as follows:

```
Line 1: 123
Line 2: 4.50 4.50
Line 3: 4
Line 4: 27 0.0 0.0 0.0
Line 5: 8 0.5 0.0 0.0
Line 6: 8 0.0 0.0 -0.5
Line 7: 57 0.5 0.5 -0.5
```

There are two differences with respect to the previous cubic case:

- now *a* and *b* are not symmetry related to *c*, so that an initial guess must be provided for both *a* and *c* (line 2).
- there are 2 kinds of independent O atoms in the cell (lines 5 and 6).

But all atoms are in special position, so that the unit cell, in spite of the number of symmetry operators, contains 5 atoms, as for SG 221.

Let us consider now SG 127, containing 2 formula units (10 atoms). Here we discover that there are at least two different ways of locating the atoms in the unit cell (corresponding to two different Wyckoff settings), which are compatible with the chemistry of perovskites (ratios 1:1:3 for La, Co, O). The two, to be described below, are here indicated as 127R and 127D, and correspond to two elementary deformations of the unit cell with respect to SG 123: In SG 127R the CoO_6 octahedra are allowed to rotate (besides the elongation or shrinking along *c*, already possible in SG 123, due to the difference between *a*, *b* and *c*). The CRYSTAL input is as follows:

```
Line 1: 127
Line 2: 5.60 4.50
Line 3: 4
Line 4: 27 0 0. 0.
Line 5: 8 0.2999 0.2001 0.
Line 6: 8 0. 0. 0.5
Line 7: 57 0. 0.5 0.5
```

Also in this case the input contains only seven *cards*. Note however that the *x* and *y* coordinates of the first oxygen can vary, in such a way that the Co-O distance in the *ab* plane remains constant, but the Co-O-Co angle along, say, *x*, is no more 180°, but

can be smaller according to the x and y coordinates in line 5.

Both Co and La are characterized by a C_{4v} point symmetry.

Among the many other possible settings, the one we indicated as 127D is of particular interest.

Line 1: 127

Line 2: 5.60 4.50

Line 3: 4

Line 4: 27 0.5 0. 0.

Line 5: 8 0. 0.5 0.5

Line 6: 8 0.75581 0.25581 0.

Line 7: 57 0.5 0.5 0.5

Note that La and Co are in special positions, which are however different from the ones in SG 127R. From the point of view of the deformation in the unit cell with respect to SG 123, here the Co point symmetry is just D_{2h} , compatible, for example, with different Co-O distances in the ab plane. The octahedra in this case are not allowed to rotate, but can deform in the two directions, say x and y. This in turn permits a different occupancy of the d orbitals in contiguous B atoms in the ab plane.

In summary, the 127R and 127D groups permit to explore independently the two most important mechanisms of modification in the unit cell, namely the octahedra rotation (OR) and the orbital

ordering (OO). The first applies in principle to all perovskites, whereas the second one to perovskites in which the t_{2g} and e_g subshells of the transition metal are partially filled. The situation for 140R and 140D is exactly the same. When additional degrees of freedom are allowed to the atoms in the unit cell, as in SG 62, then not only OR and OO can be present simultaneously, but additional rotations and octahedra deformations can take place, so that a simple interpretation of the effect of the energy lowering becomes more difficult.

Conflict of interest

The authors declare that they have no conflict of interest.

Acknowledgments

The access to the BA-HPC supercomputer facilities provided by **Bibliotheca Alexandrina** is highly acknowledged. High Performance Computing resources were partially provided by **CompSimLab** at the the Institute of Nanoscience & Nanotechnology, Kafrelsheikh University.

Authors' contribution

Conceptualization, RD, KD, KE; Data collection, AP, KE; Methodology, investigation, and data curation, KD, AP, KE, RD; collected literature then drafting the manuscript in consultation with RD, AP, KD; Review and editing, RD, KE, JS. All authors read and approved the final manuscript.

References

- Pascale F, D'Arco P, Lacivita V, Dovesi R (2021). The Superexchange mechanism in crystalline compounds. The case of KMF_3 (M= Mn, Fe, Co, Ni) perovskites. *J. Phys.: Condensed Matter*, 34, p. 074002.
- Pascale F, D'Arco P, Mustapha S, Dovesi R (2024). Orbital ordering patterns in KBF_3 (B = Sc, Ti, Fe, Co) perovskites. *J. Comput. Chem.*, 45, no. 24, 2048–2058.
- Mackrodt W, Salustro S, Civalleri B, Dovesi R (2018). Low energy excitations in NiO based on a direct Δ -SCF approach. *J. Phys.: Condensed Matter*, 30, 495901.
- Mackrodt WC, Rérat M, Gentile FS, Dovesi R (2019). An all-electron study of the low-lying excited states and optical constants of Al_2O_3 in the range 5–80 eV. *J. Phys.: Condensed Matter*, 32, p. 085901.
- Mackrodt W, Gentile F, Dovesi R (2022). The calculated energies and charge and spin distributions of the excited GR1 state in diamond. *J. Chem. Phys.*, 156, p. 044708.
- Mackrodt W, Platonenko A, Pascale F, Dovesi R (2024). The energies and charge and spin distributions in the low-lying levels of singlet and triplet N_2V defects in diamond from direct variational calculations of the excited states. *J. Chem. Phys.*, 160, 034705.
- Thornton G, Tofield B, Hewat A (1986). A neutron diffraction study of $LaCoO_3$ in the temperature range $4.2 < T < 1248$ K. *J. Solid State Chem.*, 61, no. 3, 301–307.
- Haas O, Struis R, McBreen J (2004). Synchrotron x-ray absorption of $LaCoO_3$ perovskite. *J. Solid State Chem.*, 177, no. 3, 1000–1010.
- Arima T, Tokura Y, Torrance JB (1993). Variation of optical gaps in perovskite-type 3d transition-metal oxides. *Phys. Rev. B*, 48, 17006–17009.
- Xu S, Morotomo Y, Mori K, Kamiyama T, Saitoh T, Nakamura A (2001). Structural Parameters of $LaCoO_3$ near the Spin State Transition. *J. Phys. Soc. Japan*, 70, no. 11, 3296–3299.
- Capone M, Ridley CJ, Funnell NP, Guthrie M, Bull CL (2019). High-Pressure Neutron Diffraction Study of $LaCoO_3$. *Phys. Status Solidi A*, 216, 1800736–1800740.
- Pandey SK, Khalid S, Lalla NP, Pimpale AV (2006). Local distortion in $LaCoO_3$ and $PrCoO_3$: extended x-ray absorption fine structure, x-ray diffraction and x-ray absorption near edge structure studies. *J. Phys.: Condens. Matter*, 18, 10617–10630.
- Radaelli PG, Cheong SW (2002). Structural phenomena associated with the spin-state transition in $LaCoO_3$. *Phys. Rev. B*, 66, 094408.
- Mizokawa T, Fujimori A (1996). Electronic structure and orbital ordering in perovskite-type 3d transition-metal oxides studied by Hartree-Fock band-structure calculations. *Phys. Rev. B*, 54, 5368–5380.
- Korotin MA, Ezhov SY, Solovyev I, Anisimov VI, Khomskii DI, Sawatzky GA (1996). Intermediate-spin state and properties of $LaCoO_3$. *Phys. Rev. B*, 54, no. 8, 5309–5316.

16. Sahnoun M, Daul C, Haas O, Wokaun A (2005). Investigation of the electronic structure in $\text{La}_{1-x}\text{Ca}_x\text{CoO}_3$ ($x = 0, 0.5$) using full potential calculations. *J. Phys.: Condensed Matter*, 17, 7995–8003.
17. Nohara Y, Yamamoto S, Fujiwara T (2009). Electronic structure of perovskite-type transition metal oxides LaMO_3 ($M = \text{Ti} \sim \text{Cu}$) by U+GW approximation. *Phys. Rev. B*, 79, p. 195110.
18. Knížek K, Hejtmanek J, Maryško M, Jiráček Z, Buršík J (2012). Stabilization of the high-spin state of Co^{3+} in $\text{LaCo}_{1-x}\text{Rh}_x\text{O}_3$. *Phys. Rev. B*, 85, 134401.
19. Gryaznov D, Evarestov RA, Maier J (2010). Hybrid density-functional calculations of phonons in LaCoO_3 . *Phys. Rev. B*, 82, p. 224301.
20. Yamaguchi S, Okimoto Y, Taniguchi H, Tokura Y (1996). Spin-state transition and high-spin polarons in LaCoO_3 . *Phys. Rev. B*, 53, R2926–R2929.
21. He J, Franchini C (2012). Screened hybrid functional applied to $3d^0 \rightarrow 3d^8$ transition-metal perovskites LaMO_3 ($M = \text{Sc} \sim \text{Cu}$): Influence of the exchange mixing parameter on the structural, electronic, and magnetic properties. *Phys. Rev. B*, 86, p. 235117.
22. He J, Franchini C (2014). Erratum: Screened hybrid functional applied to $3d^0 \rightarrow 3d^8$ transition-metal perovskites LaMO_3 ($M = \text{Sc} \sim \text{Cu}$): Influence of the exchange mixing parameter on the structural, electronic, and magnetic properties. *Phys. Rev. B*, 90, p. 039907.
23. Franchini C (2014). Hybrid functionals applied to perovskites. *J. Phys.: Condens. Matter*, 26, 253202.
24. Becke AD (1993). Density-Functional Thermochemistry. III. The Role of Exact Exchange. *J. Chem. Phys.*, 98, no. 7, 5648–5652.
25. Lee C, Yang W, Parr R (1988). Development of the Colle-Salvetti Correlation-Energy Formula Into a Functional of the Electron Density. *Phys. Rev. B*, 37, no. 2, 785–789.
26. Dovesi R, Saunders VR, Roetti C, Orlando R, Zicovich-Wilson CM, Pascale F, Civalleri B, Doll K, Harrison NM, Bush IJ, D'Arco P, Llunell M (2014) *CRYSTAL 2014 User's Manual*, University of Torino, Torino.
27. Dovesi R, Saunders VR, Roetti C, Orlando R, Zicovich-Wilson CM, Pascale F, Civalleri B, Doll K, Harrison NM, Bush IJ, D'Arco P, Llunell M, Causà M, Noël Y, Maschio L, Erba A, Rérat M, Casassa S (2017) *CRYSTAL17 User's Manual*, Università di Torino, Torino. <http://www.crystal.unito.it>.
28. Dovesi R, Pascale F, Civalleri B, Doll K, Harrison N, Bush I, D'Arco P, Noël Y, Rérat M, Carbonnière P, Causà M, Salustro S, Lacivita V, Kirtman B, Ferrari A, Gentile F, Baima J, Ferrero M, Demichelis R, De La Pierre M (2020). The crystal code, 1976-2020 and beyond, a long story. *J. Chem. Phys.*, 152, no. 20, p. 204111.
29. Dovesi R, Pisani C, Roetti C, Saunders VR (1983). Treatment of Coulomb Interactions in Hartree-Fock Calculations of Periodic Systems. *Phys. Rev. B*, 28, 5781–5792.
30. Causà M, Dovesi R, Orlando R, Pisani C, Saunders VR (1988). Treatment of the Exchange Interactions in Hartree-Fock LCAO Calculations of Periodic Systems. *J. Phys. Chem.*, 92, 909–913.
31. Shannon RD (1976). Revised effective ionic radii and systematic studies of interatomic distances in halides and chalcogenides. *Acta Crystallogr. Section A*, 32, 751–767.
32. Pascale F, Mustapha S, D'Arco P, Dovesi R (2023). The d orbital multi pattern occupancy in a partially filled d shell: The KFeF_3 perovskite as a test case. *Materials*, 16, 1532.
33. Pascale F, Gueddida S, Doll K, Dovesi R (2024). Band gap, Jahn-Teller deformation, octahedra rotation in transition metal perovskites LaTiO_3 . *J. Comput. Chem.*, 45, no. 10, 683–694.
34. Pascale F, D'Arco P, Dovesi R (2021). Phase transitions and superexchange mechanism in transition metal compounds. The case of KMnF_3 perovskite. *Phys. Chem. Chem. Phys.*, 23, 26780–26792.